IOSR Journal Of Applied Physics (IOSR-JAP)
e-ISSN: 2278-4861.Volume 14, Issue 5 Ser. II (Sep. – Oct. 2022), PP 12-20
www.Iosrjournals.Org

Patterning-Area Expansion of Parabolic-Mirror Projection Optics for Lithography Using One-Sided and Collimated Illumination

Toshiyuki Horiuchi[1], Jun-ya Iwasaki[1], Hiroshi Kobayashi,[1]
[1](*Advanced Machinery Engineering/ Tokyo Denki University, Japan)*

Abstract:
Background*: Wearable health monitors are noticed for effectively grasping the conditions of patients and aged peoples. And, various sensors for attaching to body parts such as lists, fingers, and chests are under developments. The sensors and their attachment parts are often made using flexible flat sheets. However, it is often better to make them on curved flexible or bendable shells or solid parts just fitting to the body parts. For this reason, a simple and low-cost method for printing 50-200 μm patterns on arbitrarily curved surfaces was invented using a magic mirror system composed of parabolic mirrors. In the past research, 200-μm L&S patterns on a transparent reticle placed at the lower mirror aperture were projected in the upper mirror aperture. However, successfully patterned areas were limited to the field center. Therefore, it is necessary to extend the patterning area to the whole exposure field.*
Studies on methods for expanding patterned areas*: At first, reasons why resist patterns were not formed in the whole field were examined by tracing the imaging light rays geometrically, and calculating projected image positions. It was found that image positions were varied depending on the illumination direction and the light ray routes, and image positions especially change at the outside parts of the exposure field. Therefore, it was thought effective to illuminate the reticle from one-side by a collimated light. So, the exposure system was renovated. The circular illumination using a ring light was changed to one-sided and collimated illumination.*
Results and Discussions*: 200-μm L&S patternswere successfully replicated in the whole exposure area of 10-mm square with a large exposure time and focus margins of±10% and ±400 μm, respectively. Practical applicability of easy and low-cost projection lithography using parabolic mirrors to patterning in common size fields was proved.*
Conclusion: *Easy and low-cost projection lithography using the parabolic mirrors will be applicable to stereophonic lithography or patterning on arbitrarily curved object surfaces with ordinary field sizes.*
Key Word*: Stereophonic lithography; Parabolic-mirror; One-sided illumination; Collimated light; Patterning area; Field distortion.*

Date of Submission: 09-10-2022 Date of Acceptance: 22-10-2022

I. Introduction

In these two decades, special lithographic technologies have been required for printing rough patterns with 10-200 μm on non-flat object surfaces easily and inexpensively. Typical targets were the patterning on cylindrical objects such as pipes, shafts, rods, and needles until quite recently.[1-11)] However, taking a step forward, patterning on gently but arbitrarily curved surfaces has begun to be required lately. Typical targets are fabrication of comfortably wearable health monitors. Health monitoring sensors for attaching to human bodies have been researched very vigorously, and various wearable biosensors are proposed.[12-17)]Body parts are not flat. So, it often becomes difficult to put the sensors and/or their wiring and power supply parts on them. For this reason, various flexible sensors and their affiliated parts are developed.[18-23)] However, because most of the flexible devices are fabricated on thin flat sheets, they are sometimes difficult to conform to irregularly curved or even twisted body parts. Therefore, it is thought that biosensors with curved shapes just fitting to the body parts are better for preventing the slipping-off and errors of sensing. Accordingly, it is preferable to use curved flexible parts just fitting to the body parts not on flat flexible sheets.

For this reason, how to print or delineate patterns on arbitrarily curved surfaces was deliberated, and a good idea of utilizing a magic mirror projection system for the stereophonic lithography occurred. It was thought that if aerial images were clearly formed on a resist film by the magic mirror projection optics, resist patterns would be formed. To realize the idea, an aperture was opened at the lower mirror bottom, and a transparent curved reticle was placed at the bottom aperture center, and illuminated obliquely upward from the

bottom. As a result, patterns on a transparent curved reticle were successfully projected at the center of the upper mirror aperture.

However, when patterning characteristics was investigated in the past research, 200-µm line-and-space (L&S) patterns were not printed except in very small areas of several mm diameter around the field center.[24-27] The pattern size of 200 µm may be felt very large compared with the sizes used for conventional applications of lithography. However, much larger patterns are used also, [23] and even the size of 200 µm is useful. On the other hand, larger patterning areas are indispensable for utilizing the stereophonic lithography practically. Therefore, reasons why patterns were not formed in the whole exposure field and how to enlarge the patterning area are discussed in this paper. It is clarified that the image position depends on where the light ray is reflected on the upper mirror, that is, the image position varies caused by the illumination light ray direction or angle. Thus, one-sided illumination of the exposure light and collimated light illumination is proposed as the new key idea for solving the problem. Patterned area is drastically enlarged to the whole exposure area. One-sided illumination by narrowly masking the ring light was tested in the past research.[28] However, using a collimated light and enabling to adjust the positions and angle of the light source, drastically improved patterning performances are exhibited here.

II. Studies On Methods For Expanding Patterned Areas

At first, results obtained in the past researches and subjects to be solved are briefly explained. Patterning characteristics of the projection optics were investigated by developing a prototype exposure system, as shown in Figure no1, and using a flat reticle and silicon wafers. As the projection optics, a magic mirror set commercially available as a scientific toy was utilized. The total diameter and the height of the toy magic-mirror set composed of a pair of parabolic mirrors were approximately 140 mm and 50 mm, respectively. As an exposure light source, the white light emitting diode (LED) ring light was used. The total sizes of the exposure system were approximately 300 mm wide, 300 mm deep, and 310 mm height.

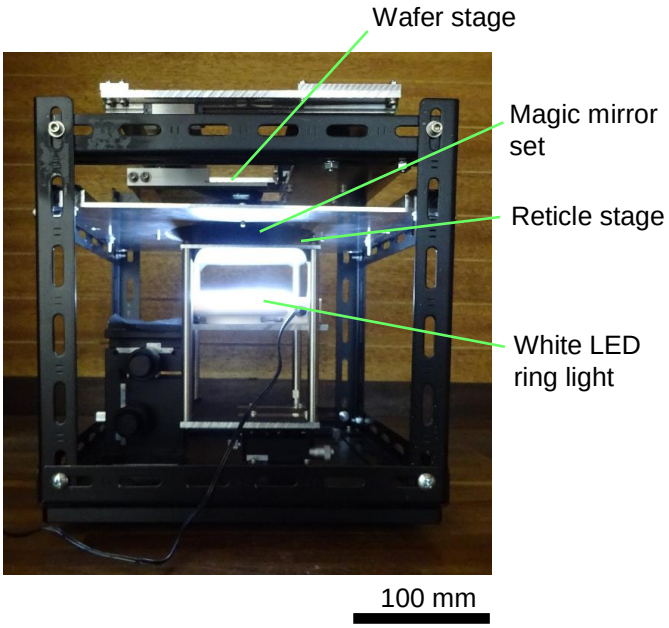

Figure no 1: Shows prototype stereophonic exposure system developed at first for investigating patterning characteristics, and clarifying subjects for realizing realistic exposure systems.

Because the mirror set was toy-use, high accuracy was not expected. In addition, fine patterning was not required for the time being. Therefore, patterning characteristics were investigated using 200-µm L&S patterns in a 10-mm square field by printing the patterns on a film reticle on 4-inch silicon wafers. However, patterns were resolved only at the center parts of the field, as shown in Figure no 2. The patterned area sizes were too small to utilize the system for the stereophonic lithography. It was thought necessary to enlarge the patterned area size so as the patterns were formed in the whole exposure field of 10 mm square first of all.Therefore, the reason why the patterned areas were limited only around the field center was discussed to enlarge the clearly patterned areas.

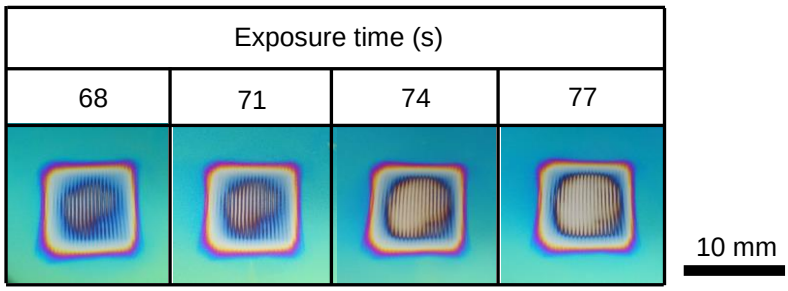

Figure no 2: Shows patterns of 200-μm L&S printed by illuminating a transparent reticle from all directions using a white LED ring light. Patterns are resolved only around the field center, and the square corners are rounded.

To clarify the reasons, travelling routes of exposure light rays passing through the point P distant x from the mirror axis on the reticle plane were traced, and the position x' of the point image P' was calculated. How to calculate the image position x' was studied and disclosed in the past research paper.[24] Values of x' calculated under various light route conditions were also reported. However, the illumination directions were not considered sufficiently, and it was newly found here that the image positions x'_r and x'_{-r} formed by the light rays reflected on the right and left parts of the upper mirror differed each other, even if the radial positions r and $-r$ of the reflection points A and B were same, as shown in Figure no 3. It is essential to coincide the image positions x'_r and x'_{-r} for forming clear images on the image plane.

Next, image position differences for slightly different light routes were calculated, as shown in Figure no 4. As a result, it was found that the image position x' shifted from x_1' to x_2', and to x_3' depending on the radial positions r_1, r_2, and r_3 of the reflected points on the upper mirror.

Thus, numerical relationships between the reticle pattern position x and the image positions x'_r and x'_{-r} and their dependence on the radial positions of r and $-r$ was calculated, as shown in Figure no 5.

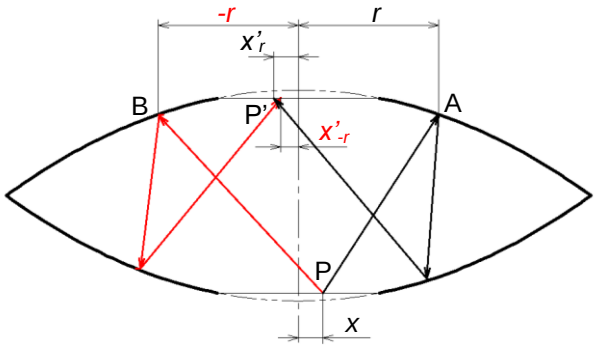

Figure no 3: Shows the exposure light rays traced in the opposite directions. Position differences of images formed by light rays illuminated from opposite directions were calculated.

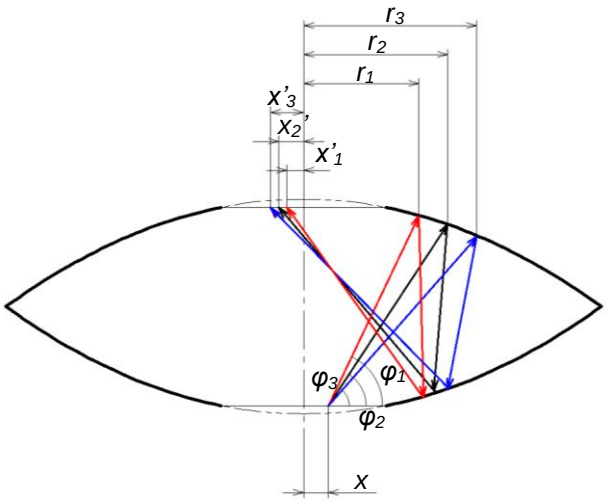

Figure no 4: Shows position differences of images formed by light rays illuminated by different angles of φ_1, φ_2, and, φ_3 were calculated. Reflected position of r_1, r_2, and r_3 were used as the calculation parameters actually.

It was thought that expansions and shrinks of the exposure field are expressed by $(|x'|-|x|)$. For this reason, relationship between the image position shifts $(|x'|-|x|)$ and the reticle pattern position x was calculated, next. The results are shown in Figure no 6.

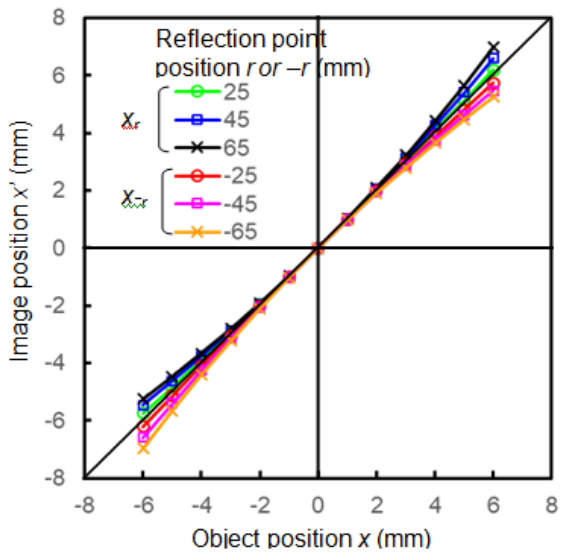

Figure no 5: Shows relationships between the reticle pattern position x and the image positions x'_r and x'_{-r}, and their dependence on the radial positions of r and $-r$.

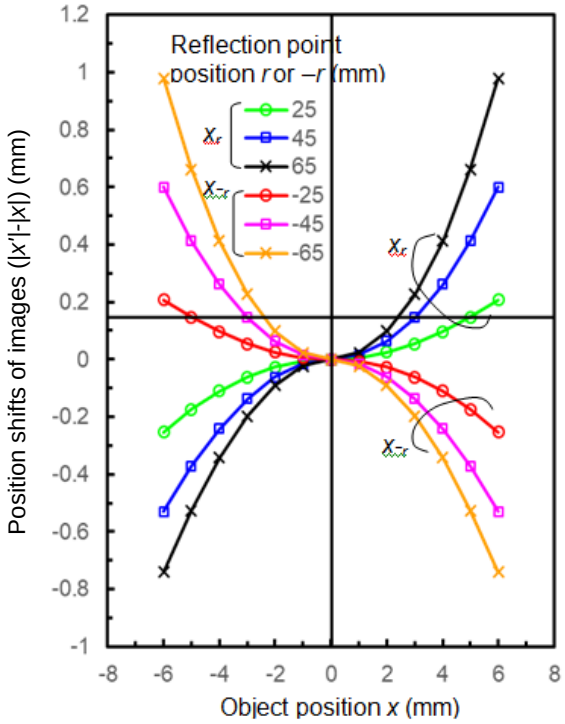

Figure no 6: Shows relationships between the image position shifts ($|x'|-|x|$) and the reticle pattern position x. The image position shifts cause expansions and shrinks of the exposure field and pattern sizes.

It was clarified that the expansion and shrinkage of the field were switched by the directions of illumination light rays. The difference between x'_r and x'_{-r} becomes significant when x_r and x_{-r} are large. That is, x'_r and x'_{-r} differs greatly at the outside parts of exposure field. Accordingly, caused by the image shifts arose out of the illumination from various directions, total images are blurred at the outside parts of the exposure field. Therefore, the illumination should be limited from one side to realize the patterning in a large field. It was also clarified that because image positions depended on where each ray was reflected on the upper mirror, illumination light ray directions should be restricted in narrow angles or unified. Thus, it was thought effective to use a collimated light for unifying the illumination light ray routes. Based on these considerations, it was concluded that the one-sided illumination toward the optimum direction using a collimated light would be the best answer for preventing the image blurs at the outside parts of field and drastically expanding the patterned area to the whole exposure field.

III. Patterning Results Using One-sided And Collimated Illumination

In the previous section, it was clarified that one-sided illumination using a collimated light would be effective to expand the patterning area and improve the resolution. For this reason, the effects were actually tested by renovating the prototype exposure system shown in Figure no 1, and attaching a collimated LED light. Figure no 7 shows the renovated exposure system. The white LED ring light was removed, and a collimated LED light (Dynatec, LBF-LX60AAUV-405) was placed instead. The central wavelength of the LED was 405 nm. Because the light ray angle φ shown in Figure no 4 should be adjusted suitably, mechanisms for moving the light in horizontal and vertical directions, and adjusting the inclination angle φ were equipped.

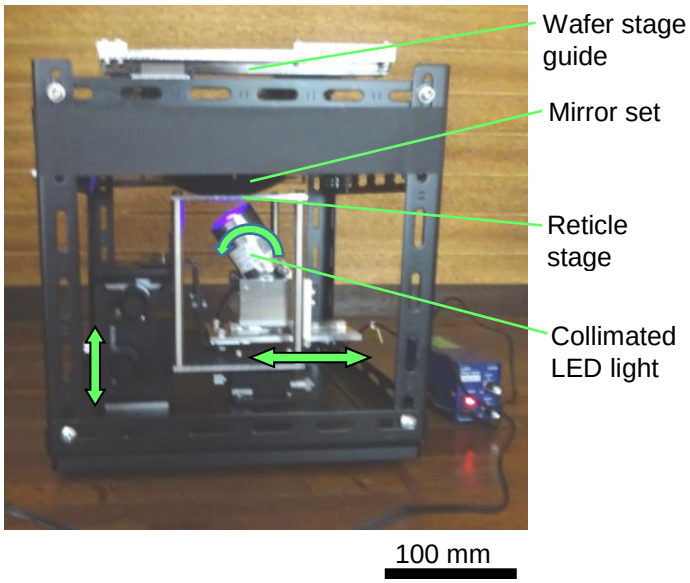

Figure no 7:Shows exposure system renovated by equipping a collimated blue LED light. Positions and inclination angle are arbitrarily adjustable.

The optimum position and angle of the collimated light were adjusted by placing a sheet of tracing paper instead of a wafer on the fork of wafer stage. The tracing paper sheet worked as a diffuser, and light intensity distribution of the pattern images were reproduced, as shown in Figure no 8. It was found that the patterning performances were predictable by the clearness and edge definition of the pattern images projected on a tracing paper sheet.

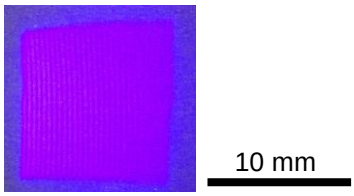

Figure no 8: Shows pattern images projected on a tracing paper sheet placed instead of a wafer.

Printed 200-µm L&S patterns under the conditions of various exposure times and focal positions are shown in Figure no 9 and Figure no10, respectively. It was verified that resist patterns were printed without blurs in the whole exposure field including the outside parts. Printed pattern shapes did not change much for the variations of exposure time and focal position. The upper right slashed parts were produced by the unwilling turning up of the black tape holding the reticle edge.

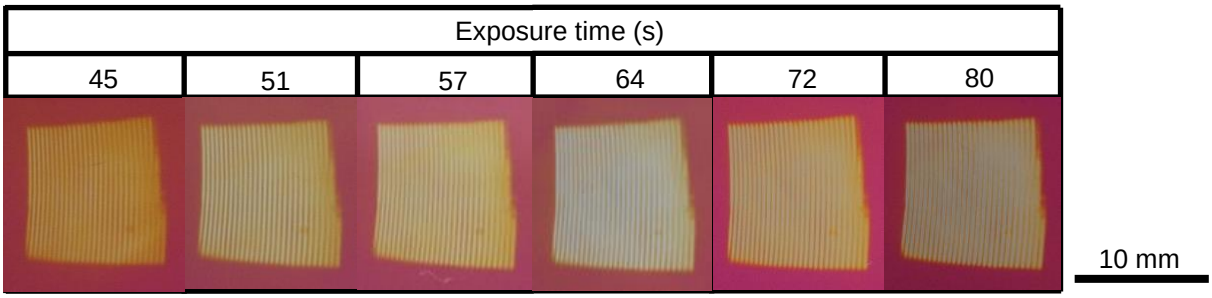

Figure no 9: Shows slight changes of 200-µm L&S resist patterns for exposure time variation.

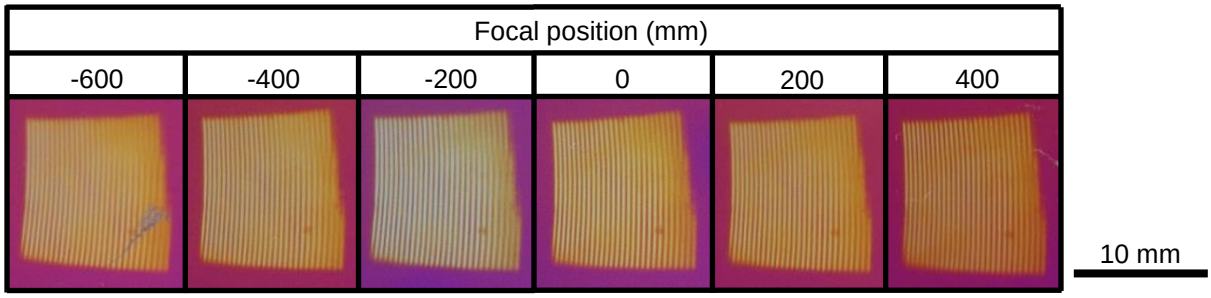

Figure no 10: Shows stability of 200-µm L&S resist patterns for the change of focal position.

Figure no 11 shows the resist pattern width dependence on the exposure time. The width changed within ±10% for the ±10% change of exposure times. Fairly large exposure time margin was obtained. On the other hand, Figure no 12 shows the resist pattern width dependence on the focal position. The width changed within almost ±10% for the focal position change of ±400 µm. It was clarified that the focus margin was strikingly large.

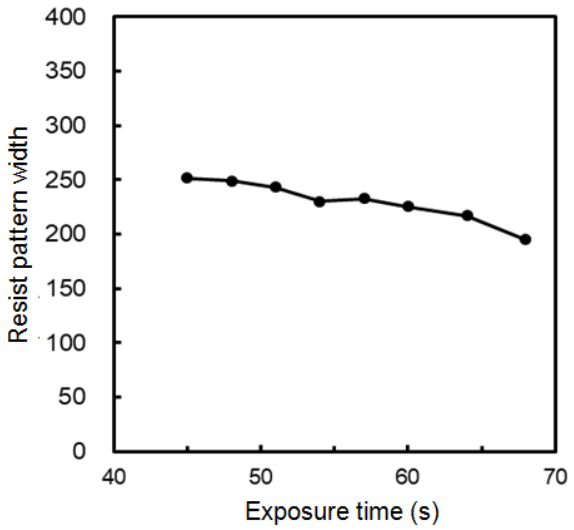

Figure no 11: Shows relationship between the resist pattern width and exposure time.

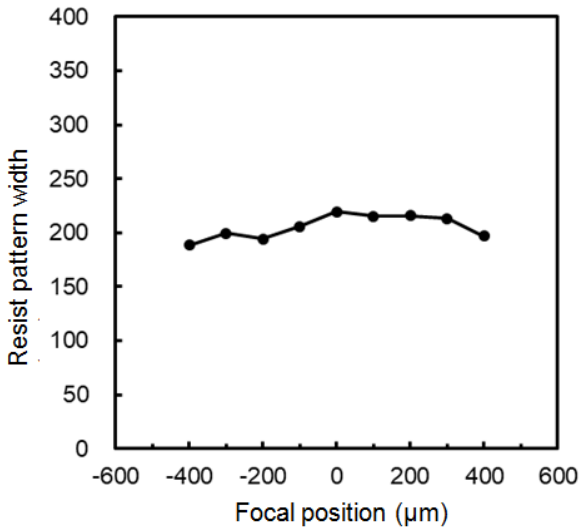

Figure no 12: Shows relationship between the resist pattern width and the focal position.

IV. Discussion

Although even if the illumination light angle is unified by using a collimated light, it was thought that diffracted light rays arose from the fine patterns on the reticle object. For this reason, spread of light rays by the diffraction was checked, and feasibility of resolution improvement down to 50-100 µm sizes in the near future was discussed.

The diffraction angle θ for periodical line patterns is calculated by eq. (1).

$$\theta = \sin^{-1}(\lambda/p). \qquad (1)$$

Here, λ is the wavelength and p is the pattern pitch.

If the aimed minimum pattern size is 50 µm, and main wavelength of the collimated LED is 405 nm, θ is calculated as shown in eq. (2) by substituting p=100 µm and λ=0.405 µm in eq. (1).

$$\theta = 0.00405 \text{ rad} = 0.232°. \qquad (2)$$

The distance d between the original object placed at the aperture center of lower mirror to the reflection point on the upper mirror is roughly estimated almost equal to the height of mirror set, and is estimated approximately d=50 mm. Accordingly, the change of reflection point position $\triangle r$ for the diffracted light is calculated by

$$\triangle r = d\theta \cos 45° = 0.143 \text{ mm}, \quad (3)$$

if the light ray angle φ shown in Figure no 8 is assumed to be φ=45°.

Image position shift (x'-x) dependence on the reflection point position r was plotted as shown in Figure no13 for the case of x=5 and x=4 corresponding to the exposure field size of 10 and 8 mm square. Because (x'-x) changes almost linear to the reflection point position r, change of image position shift $\triangle(x'$-$x)$ dependence on the reflection point position change $\triangle r$ is roughly estimated when x=5, as shown in eq. (4).

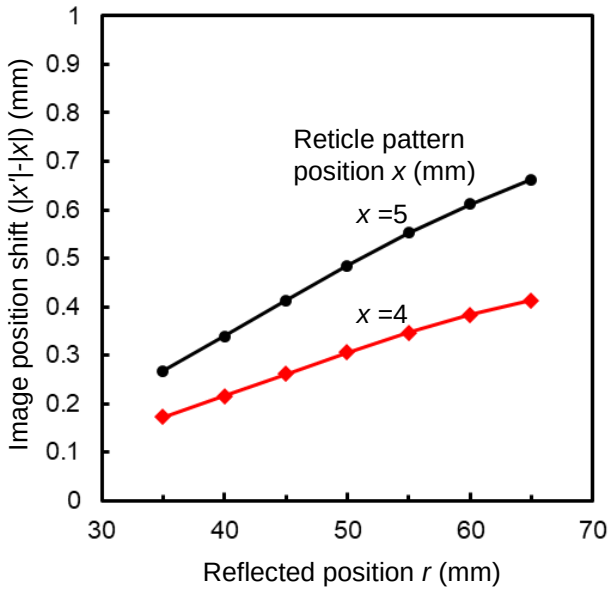

Figure no 13: Shows relationship between image position shift and reflected position.

$$\triangle(x'\text{-}x) / \triangle r = (0.662\text{-}0.268) \text{ mm} / (65\text{-}35) \text{ mm} = 0.013. \quad (4)$$

Therefore, the image position shift $\triangle(x'$-$x)$ caused by the diffracted light rays is calculated by substituting eq. (3) to eq. (4).

$$\triangle(x'\text{-}x) = 0.013 \times 0.143 \text{ mm} = 1.8 \text{ µm}. \quad (5)$$

The diffraction angle θ shown in eq. (2) and the shift of image positions shown in eq. (5) are very small values. Therefore, it is thought that the diffraction light does not almost affect the resolution of large patterns treating here. Though the plastic toy mirrors with poor accuracy were used, 200-µm L&S patterns were clearly resolved this time. Because influence of diffracted light was estimated to be very small, printing of 50-100 µm L&S patterns will be probably possible, if mirrors fabricated as regular optical components are equipped, and the illumination light is collimated almost in parallel.

On the other hand, the image contrast is also degraded by other factors such as light dispersion from reticle pattern edges, and surplus exposure by the light wrongly illuminates the exposure field without being reflected by the mirrors. These unfavorable matters may be cared also.

V. Conclusions

To secure the practicability of the stereophonic lithography using the magic mirror optics, enlargement of patterned area in the whole exposure field was aimed. At first, why the patterned areas were limited only in a small one around the exposure field center was clarified by tracing the light rays. In concrete, illumination light rays passing through a point on the original reticle and going to the image plane were traced, and relationship between the reticle and image pattern positions was clarified.

As a result, it was newly found that positions of pattern images formed by the illumination light from opposite directions, for example, from right and left differ considerably each other. The image position difference increases as the original reticle pattern position separates distant from the field center. Accordingly, when the original reticle was illuminated from all directions by a ring light in the past research, it was thought pattern images formed at variously shifted positions were superimposed, and totally formed images were blurred, especially at the outside parts of the field.

It was also found that the image position depends on the light route. That is, it depends on the reflection point position r on the mirror or the inclination angle φ of the light ray. For this reason, if the reticle is illuminated by a widely emitted light, light rays are dispersed on the image plane, and pattern images are blurred.

Based on these studies, one-sided illumination by a collimated LED was adopted, and the exposure system was renovated. As a result, 200-μm L&S patterns were successfully replicated in the whole 10-mm square exposure field. The exposure time margin was as long as ±10%, and the focus margin was as large as nearly ±400 μm. The pattern width of 200 μm is thought very large comparing with the sizes used in conventional lithography applications. However, it is useful for the new applications. For example, much wider or larger patterns are used as wiring patterns and electrode pad patterns.[23)]

On the other hand, it may be thought unfavorable that the exposure fields were distorted to warped trapezoids when the new illumination method is applied. However, the distortions are not serious problems. Because the articles to be patterned are warped or deformed from the beginning, distortions are anticipated in advance, and necessary articles are designed as the distortions are permissible to some extent. In addition, systematic or regular deformations can be compensated by modifying the reticle patterns, if necessary. Only good patterning repeatability should be secured for enabling alignments with other patterning layers.

At the present stage, the resolution limit and the exposure field distortion are not so important items as the practical applicability of the easy and low-cost projection lithography to arbitrarily curved articles with common sizes. In addition, both improvement of resolution and compensation of distortions will be responded in the futureafter the basic practicability is proved.

Acknowledgement

This work was partially supported by JSPS KAKENHI 20K05293 and a Grant from Shonan Instruments.

References

[1]. X. Haoa, L. Wanga, Q. Wanga, F. Guoa, Y. Tanga, Y. Dinga, B. Lua, Surface micro-texturing of metallic cylindrical surface with proximity rolling-exposure lithography and electrochemical micromachining. Applied Surface Science.2011; 257: 8906-8911.
[2]. D. Lee, H. Hiroshima, Y. Zhang, T. Itoh, R. Maeda, Cylindrical projection lithography for microcoil structures. Microelectronic Engineering. 2011; 88: 2625–2628.
[3]. H. Lim, K. Choi, G. Kim, S. Lee, H. Park, J. Ryu, S. Jung, J. Lee, Roll-to-roll nanoimprint lithography for patterning on a large-area substrate roll. Microelectronic Engineering. 2014; 123: 18–22.
[4]. S. Chun Tseng, W. Y. Peng, Y. F. Hsieh, P. J. Lee, W. L. Lai, Electron beam lithography on cylindrical roller. Microelectronic Engineering. 2010; 87: 943–946.
[5]. U. Tahira, M. A. Kamrana, M. H. Janga, M. Y. Jeong, Thin-film coating on cylinder for fabrication of cylindrical mold: Roll-to-roll nano-imprint lithography. Microelectronic Engineering. 2019; 211:5-12.
[6]. T.Horiuchi, T.Furuhata, and H.Muro, Synchronous scan-projection lithography on overall circumference of fine pipes with a diameter of 2 mm. Japanese Journal of Applied Physics. 2016; 55: 06GP13.
[7]. T.Horiuchi, K. Nakamura, Scan-projection optical lithography onto cylindrically curved convex and concave surfaces with inhomogeneous curvature radii. Microelectronic Engineering. 2011;88: 2563-2566.
[8]. T.Horiuchi, K. Ito, Y. Suzuki, A.Yanagida, and H. Kobayashi, Fabrication of Stent-Like Mesh Structures Using Synchronized Scan Rotation Lithography and Wet Etching.Journal of Photopolymer Science and Technology. 2020; 33: 361-367.
[9]. T.Horiuchi, H. Ishii, Y. Shinozaki, T. Ogawa, and K. Kojima, Novel Fabrication Method of Microcoil Springs Using Laser Scan Helical Patterning and Nickel Electroplating. Japanese Journal of Applied Physics.2011; 50: 06GM10.
[10]. T. Horiuchi, H. Sakabe, and H. Kobayashi, Patterning of Multi-slits on Pipes for Developing Fine Diameter Stents, Proceedings. Proceedings of BIODEVICES 2015; Lisbon, Portugal: 103-108.
[11]. H. Takahashi and Toshiyuki Horiuchi, Laser-Scan Lithography and Electrolytic Etching for Fabricating Meshed Pipes of Stainless Steel. Journal of Photopolymer Science and Technology. 2018; 31(1): 51-57.
[12]. H. Zheng, H. Chen, Z. Pu, D. Li, A breathable flexible glucose biosensor with embedded electrodes for long-term and accurate wearable monitoring.Microchemical Journal. 2022; 181: 107707.
[13]. M. A. Komkova, A. A. Eliseev, A. A. Poyarkov, E. V. Daboss, P. V. Evdokimov, A. A. Eliseev, A. A. Karyakin, Simultaneous monitoring of sweat lactate content and sweat secretion rate by wearable remote biosensors. Biosensors and Bioelectronics. 2022; 202: 113970.
[14]. X. Zeng, R. Peng, Z. Fan, Y. Lin, Self-powered and wearable biosensors for healthcare. Materials Today Energy. 2022; 23: 100900.
[15]. X. Gong, K. Huang, Y. H. Wu, X. S. Zhang, Recent progress on screen-printed flexible sensors for human health monitoring. Sensors & Actuators: A. Physical.2022; 345: 113821.
[16]. D.Kukkar, D. Zhang, B.H. Jeon, K. H. Kim, Recent advances in wearable biosensors for non-invasive monitoring of specific metabolites and electrolytes associated with chronic kidney disease: Performance evaluation and future challenges. Trends in Analytical Chemistry.2022; 150: 116570.
[17]. A.Reda, S. A. E. Safty, M. M. Selim, M. A. Shenashen, Optical glucose biosensor built-in disposable strips and wearable electronic devices. Biosensors and Bioelectronics. 2021; 185: 113237.
[18]. D. T. Phan, T. T. V. Phan, T. C. Huynh, S. Park, J. Choi, J. Oh, Noninvasive, Wearable Multi Biosensors for Continuous, Long-

term Monitoring of Blood Pressure via Internet of Things Applications. Computers and Electrical Engineering. 2022; 102: 108187.
[19]. C.V.Anikwe, H.F.Nweke, A.C.Ikegwu, C.A.Egwuonwu, F.U.Onu, U.R.Alo, Y.WahTeh, Mobile and wearable sensors for data-driven health monitoring system: State-of-the-art and future prospect. Expert Systems with Applications.2022; 202: 117362.
[20]. D.Verma, K. RB Singh, A. K. Yadav, V.Nayak, J. Singh, P. R. S. R. P. Singh, Internet of things (IoT) in nano-integrated wearable biosensor devices for healthcare applications. Biosensors and Bioelectronics. 2022; 11: 100153.
[21]. A. Nag, R. B.V.B. Simorangkir, D. R. Gawade, S.Nuthalapati, J. L. Buckley, B.O'Flynn, M. E. Altinsoy, S.C.Mukhopadhyay, Graphene-based wearable temperature sensors: A review. Materials & Design. 2022; 221: 110971.
[22]. X.Jin, G. Li, T. Xu, L. Su, D. Yan, X. Zhang, Fully integrated flexible biosensor for wearable continuous glucose monitoring. Biosensors and Bioelectronics. 2022; 196: 113760.
[23]. P. Zhu, H. Peng, A. Y. Rwei, Flexible, wearable biosensors for digital health. Medicine in Novel Technology and Devices.2022; 14: 100118.
[24]. T. Horiuchi and H. Kobayashi: Stereophonic Projection Exposure Using a Pair of Parabolic Mirrors.Digest of Papers, Photomask Japan 2021 (Yokohama, Japan).2021; p. 21.
[25]. T. Horiuchi and H. Kobayashi, Stereophonic projection lithography using parabolic mirrors. Proceedings of SPIE.2021; 11908: 1190808.
[26]. T. Horiuchi and H. Kobayashi, INVESTIGATION OF PROJECTION EXPOSURE SYSTEM USING A PAIR OF PARABOLIC MIRRORS. Abstract of MNC 2021 (On-line, Japan).2021; 29A-3-4.
[27]. T. Horiuchi and H. Kobayashi, Feasibility of stereophonic projection lithography applying a parabolic magic mirror system. Japanese Journal of Applied Physics.2022; 61: SD1042.
[28]. T. Horiuchi, J. Iwasaki, and H. Kobayashi, Stereophonic Lithography Using a Parabolic Mirror Projection System and One-sided Illumination, Technical Digest, ODF'22 (Sapporo, Japan). 2022; OThA4A-03.

Toshiyuki Horiuchi, et. al. "Patterning-Area Expansion of Parabolic-Mirror Projection Optics for Lithography Using One-Sided and Collimated Illumination." *IOSR Journal of Applied Physics (IOSR-JAP)*, 14(5), 2022, pp. 12-20.